TOP QUARK STUDIES AND IMPLICATIONS FOR FINDING NEW PHYSICS AT THE TEVATRON

Raymond E. Hall*
Department of Physics
California State University, Fresno, CA 93710

Representing the DØ and CDF Collaborations

ABSTRACT

The top quark was discovered in 1995 by the CDF and DØ collaborations in $p\bar{p}$ collisions at the Tevatron collider, which delivers a center of mass energy of 1.8 TeV. Since then, each experiment has collected a total of roughly 100 top quark candidate events and from these limited statistics comes all experimental knowledge of top quark properties. With five separate measurements between these two experiments the top quark mass is now measured to $\delta\, m_t$ = 2.9%, the most precisely known of all the quark masses. Due to its curiously heavy mass there is hope that the top may be different in other ways that might point to new physics beyond the Standard Model. The Standard Model predicts many other properties of the top quark, including its production and decay, and these proceedings will survey the measurements made with the current data set to see if there is any hint of deviation from Standard Model expectations and hence discovery of new phenomena. The large mass of the top quark also allows CDF and DØ to make indirect measurements of intrinsic spin of a bare quark, and to verify the V-A coupling in its decay to a real W boson. We also look for evidence of predicted single top production and possible competing production processes such as charged Higgs production. Finally we look to the improvement to all these measurements that the upcoming Run II of the Tevatron promises.

1 Top Quark Search and Discovery

Within the current Standard Model, the building blocks of matter are the three generations of fermions. The search for top was ushered in by the discovery in 1977 of the bottom quark, first evidence of a third generation of quarks, seen in a fixed target experiment at Fermilab.[1] With little hint from the Standard Model (SM) on what the top quark mass should be, many years were spent increasing accelerator energies and simultaneously raising the lower limit on the top quark's mass. Finally by 1990, while sitting at the Z^0 resonance, the SLAC[2] and LEP[3] e^+e^- colliders had produced no top quarks among the decay of any Z Bosons. This set a lower limit on the mass of the top of $m_t > 46$ GeV/c^2 at a 95% confidence level, or larger than half the Z boson mass.

At the same time indirect evidence for the existence of the top quark was mounting. The most compelling evidence was the confirmation that the bottom quark has the weak isospin quantum number (I_3^b) of -1/2, exactly what the Standard Model requires for the bottom quark to be in a doublet with the top as its partner. This was determined from four complementary measurements: the forward-backward asymmetry[4] in $e^+e^- \rightarrow b\bar{b}$, the absence of flavor-changing neutral currents in bottom quark decays[5,6] , the absence of large tree level $B_d^0\bar{B}_d^0$ mixing[7,8] , and the Z^0 partial decay width into $b\bar{b}$ pairs.

In addition, there also became available many precision measurements of electroweak parameters in the SM. It turns out that the Standard Model provides many indirect constraints on m_t through measurements that are sensitive to box diagrams ($B_d^0\bar{B}_d^0$ mixing), or radiative corrections (to the W and Z boson masses) which include m_t in the one loop diagrams. By using data from LEP, SLC and νN scattering data, and an estimated range of Higgs mass (M_H), the LEP electroweak working group[9] found that SM assumptions on the above mention processes led to a fitted top quark mass of

$$m_t = 178^{+11}_{-11}(stat)^{+18}_{-19}(syst) \text{ GeV/c}^2. \tag{1}$$

The search then shifted to the more powerful $p\bar{p}$ machines, most importantly the Tevatron $p\bar{p}$ Collider at Fermilab with a center of mass energy of 1.8 TeV, which today still has the highest available collision energy. With the above experimental and theoretical lower limits on m_t , the search signal had become well defined. With the top mass greater than that of the W Boson, pair production would dominate, and its subsequent decays would produce very energetic daughters. In fact with m_t in this range the standard model decay of the top is to a bottom quark and a real W boson. The topology of the event then is determined by the subsequent decay of these two W bosons. The

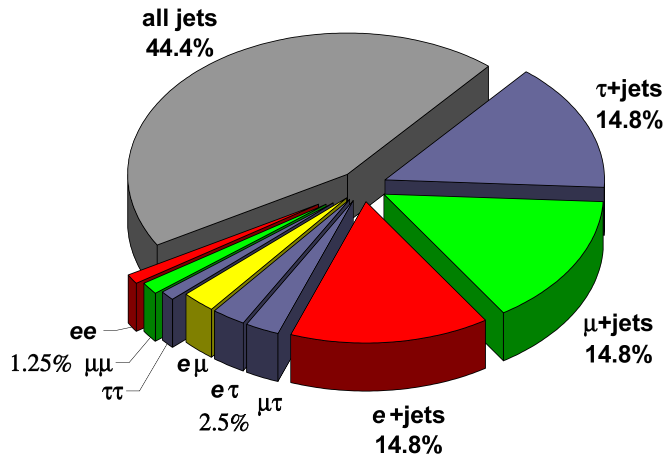

Fig. 1. Branching fraction of a $t\bar{t}$ pair to various final state signatures

decay branching fractions of the W boson are well measured, so with a little algebra we can determine how often a $t\bar{t}$ decay will feature an isolated high p_T lepton in the final state. Figure 1 summarizes the signature decay channels of top pairs which are named according to the daughter leptons from the W boson decays involved. The $dilepton$ channels are those where both W bosons decay to leptons; ee, $\mu\mu$, and $\tau\tau$ are each 1.25% of all $t\bar{t}$ decays, and $e\mu$, $e\tau$ and $\mu\tau$ each comprise 2.5% of all $t\bar{t}$ decays. The $lepton + jets$ channels (one W boson decays to $e\nu$, $\mu\nu$, or $\tau\nu$, and the other to a two jet final state) each make up 14.8% of all $t\bar{t}$ decays. The remaining 44.4% of $t\bar{t}$ decays are from the *all-jets* channel, where both W bosons decay to two-jet final states.

The top quark was finally discovered simultaneously by the CDF[10] and DØ[11] collaborations in 1995 based on a data sample of roughly 60 pb^{-1} for each experiment. The top turned out to be very heavy indeed, and even with collisions at 1.8 TeV the production of top pairs was a very rare process, and to find it entailed a sum of search analyses over all the possible decay signatures.

2 The CDF and DØ Detectors: How to catch a top quark

The daughter W bosons from top decays can result in either high transverse momentum (p_T) leptons or quarks. The daughter b-quarks form jets of hadrons and are also high in p_T. The search for top then entails the detection of the decay of these daughter W bosons and b-quarks.

The detection of W bosons daughters focuses on the leptonic decays $W \to e\nu$ and $W \to \mu\nu$, and to a lesser extent $W \to \tau\nu$ due to difficulties in reconstruction of the τ. The DØ[12] and CDF[13] detectors both have central charged particle tracking detectors and finely segmented sampling calorimeters to detect and measure high p_T electrons. Both detectors are surrounded by proportional drift tube chambers to capture high p_T muons. Both experiments detect the presence of neutrinos through the imbalance of energy in the detector (through assumption of momentum conservation in the plane transverse to the beam), a technique that relies on full coverage and hermetic calorimeters and muon detectors. Decays of W bosons to quarks are also detected with the sampling calorimeter.

The b-quarks are identified by two methods. The first method of 'tagging' the b-quark is based on detection of low p_T muons. Based on the semileptonic branching fractions, approximately 18% of all b-quarks will produce a muon in the final state. Thus a b-quark decay will result in a hadron jet measured in the calorimeter with a low p_T muon coming out the back, a configuration which is detectable with high efficiency. This method is used by both experiments.

The second method is to take advantage of the 1.6 ps lifetime and high p_T of the b-quark. The decay vertex of a b-quark will be displaced by about 0.5 cm from the primary collision vertex. A precise charged particle tracker, such as the CDF silicon based SVX,[14] can locate these displaced vertices and thereby identify the b-quarks.

3 Initial Measurements: Pair Production Cross Section and Mass

3.1 Counting experiments

To discover the top quark we must detect events that fit the $t\bar{t}$ pair decay hypothesis. A complication is that there are of course background processes that can mimic the event characteristics (collectively referred to as the topology of the event) of $t\bar{t}$ decays. The dilepton channels have the least competing background processes, which somewhat compensates for their small branching fraction. The $e\mu$ channel is referred to as the 'golden channel' as the main background is primarily W boson pair production with associated jets, a process with a cross section smaller than that of $t\bar{t}$ production. The dilepton channels ee and $\mu\mu$ have the additional background of Z boson plus associated jets production. Fortunately this background can be severely reduced by cutting out events where the invariant mass of the lepton pair is near the mass of the Z boson.

Table 1. Number of $t\bar{t}$ candidate events observed and background events expected in the absence of $t\bar{t}$ production.

experiment	DØ		CDF	
dilepton channel	$ee, e\mu, \mu\mu$		$ee, e\mu, \mu\mu$	$e\tau, \mu\tau$
number of events	9		9	4
background	2.6 ± 0.6		2.4 ± 0.5	2.0 ± 0.4
lepton+jets channel	topological	muon b-tag	vertex tag	muon b-tag
number of events	19	11	29	25[a]
background	8.7 ± 1.7	2.4 ± 0.5	8.0 ± 1.0	13.2 ± 1.2
all jets channel				
number of events	41		187	
background	24 ± 2.4		151 ± 10	

[a] some events are in both the CDF vertex tag and muon b-tag event sets

The lepton+jets channel is the second best in terms of signal to background, and the higher branching fraction gives better statistics. It is also important to find this channel because, as detailed in the next section, the presence of only one neutrino allows the mass of the two top quarks to be reconstructed with a 2C fit. The primary backgrounds to the lepton+jets channel is the production of W bosons with associated jets and to a lesser extent QCD multijet production where one jet is misidentified as an electron. Although it is rare for a W boson be produced with four jets (as in the $t\bar{t}$ decay) the cross section for W bosons to be produced with this much p_T is greater than the cross section of $t\bar{t}$ production. Figure 2 show a histogram of the W + jets background events as a function of number of jets above 15 GeV for roughly 80 pb^{-1} of data.

Three methods have been developed to separate the $t\bar{t}$ from these backgrounds. The topological analysis selection developed by DØ takes advantage of the fact that a $t\bar{t}$ pair is predominantly produced near rest and that the decay of two such massive bodies produces a spray of particles which is, on average, quite uniformly spherical in distribution. Two variables which can separate signal from background are H_T (defined as the scalar sum of all the jet transverse energies) which is said to be analogous to the 'temperature' of the event, and aplanarity, $\mathcal{A}$, which is the lowest term of the momentum

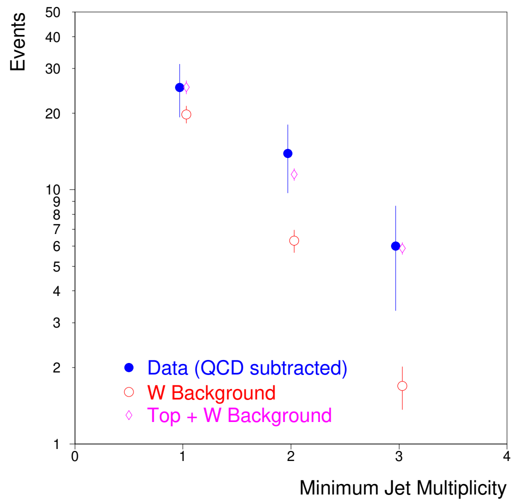

Fig. 2. Number of muon tagged μ + jets events as a function of inclusive number of jets in the event with $E_T > 15$ GeV. The excess due to $t\bar{t}$ production over the W + jets background is seen clearly for the events with three or more jets.

tensor and depicts how spherically symmetric the event products are distributed. The other two methods depend on the identification of b-quarks through the tagging methods describe earlier. Both CDF and DØ use soft muon b-tagging and CDF uses the very elegant technique of vertex b-tagging utilizing their silicon based particle tracker the SVX.

The analyses to detect decay channels that involve taus are more complex and utilize the precision charged particle tracking of CDF.[15] Due to the complexity and inefficiency of identifying taus the signal to background is inferior to the above-mentioned channels.[18] Finally there is the all-jets channel, the six jet final state, where the overwhelming background is QCD multijet production. The discrimination of $t\bar{t}$ events from this background is accomplished on larger statistical samples using a combination of the b-tagging techniques[20] and multivariate and/or neural net analyses.[19] Table 1 lists the number of events found in the DØ and CDF data along with the calculated expected backgrounds, broken down by the described decay channels.

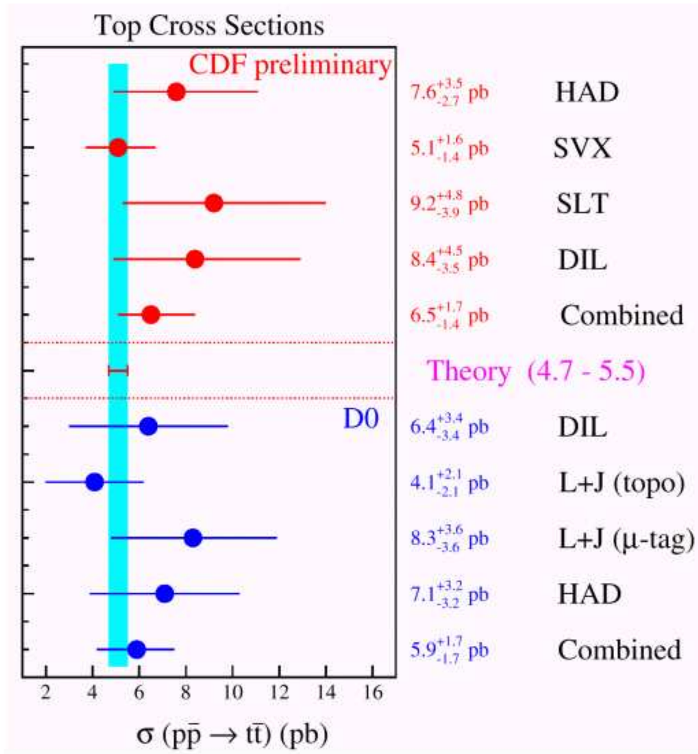

Fig. 3. Cross sections

3.2 Top Quark Pair Production Cross Section

A measurement of the $t\bar{t}$ cross section enables a test of QCD at the high mass scale associated with the top quark ($Q^2 \sim m_t^2$). The acceptances of the DØ and CDF detectors scale as a function of top quark mass since the distributions of lepton p_T and jet E_T spectra change as m_t increases. Thus the $t\bar{t}$ production cross section, $\sigma_{t\bar{t}}$, is determined as a function of m_t from the number of observed events in each of the decay channels. So for a given channel:

$$\sigma_{t\bar{t}} = \frac{N_{obs} - B}{A\mathcal{L}}$$

where N_{obs} is the number of observed events, B is the number of expected background events, A is the total acceptance$\times$efficiency, and $\mathcal{L}$ is the integrated luminosity.

The measured cross sections from the two experiments[16,17] are listed and plotted with relative errors in Figure 3. This figure also demonstrates the agreement of the separate analysis channels as listed in Table 1. Be cautioned that each experiment reports their cross section measurement for a different value of m_t (the respective measured value of each experiment) and thus a true comparison of central values is not possible

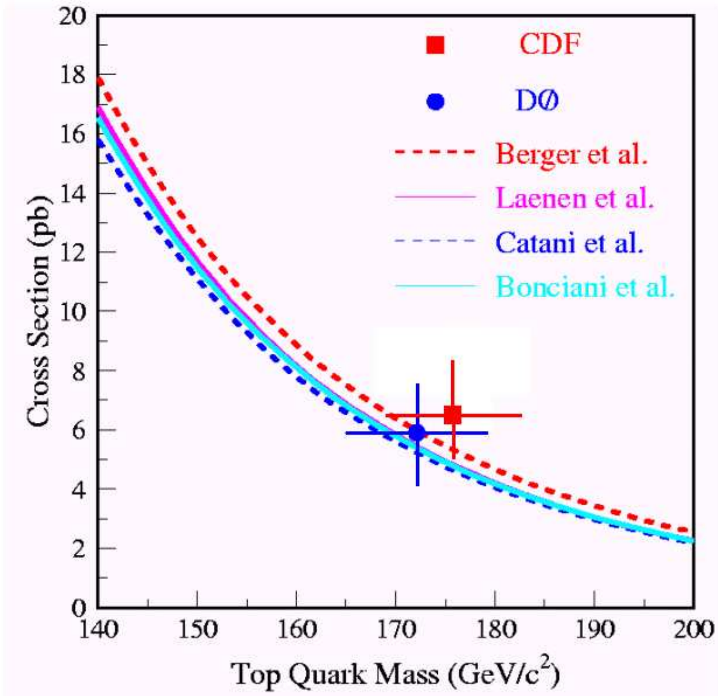

Fig. 4. Measured cross section ($\sigma_{t\bar{t}}$) for DØ and CDF (points with errors) and four theoretical NNLO calculations (lines).

with Figure 3. A true comparison of the measured cross sections is made on a plot of pair production cross section versus top mass as in Figure 4. Also shown are curves from four pertubative (NNLO) QCD calculations[21] to provide comparison to theoretical expectations (authors cited in figure).

3.3 Methods of top mass determination

Both experiments have made multiple measurements of the top quark mass through a variety of techniques and event data samples. The most straight forward of these is a two-constraint kinematic fit which reconstructs the top and antitop masses from the lepton+jet event samples.[22,23]

Eighteen quantities define the kinematics of the six particle final state of a $t\bar{t}$ decay, all of which can be measured with the exception of one; the momentum component of the neutrino along the beam axis. However, the fit can take advantage of three constraints: 1) the charged lepton and missing E_T are constrained to the mass of the W boson, 2) two jets are selected to constrain to the second W boson mass, and 3) each reconstructed W is paired with a remaining jet (which then represents the t and $\bar{t}$

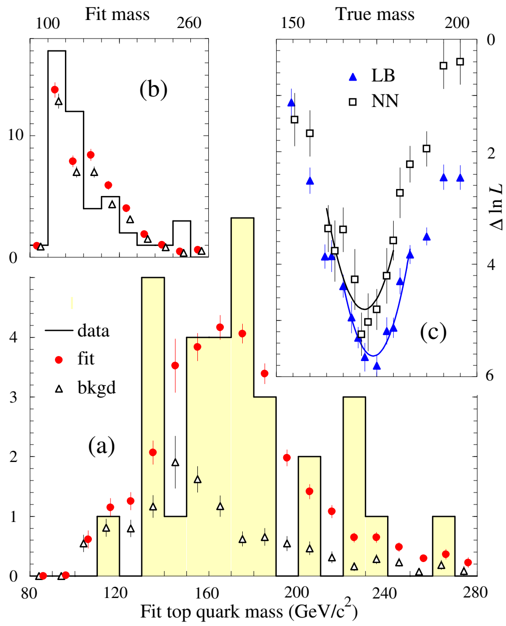

Fig. 5. The 2C, two-dimensional binned likelihood fit of the DØ lepton+jets events giving a top mass of 173.3±5.6 (stat) ±5.5 (sys) GeV/c^2

quark masses) and the final constraint is that these reconstructed t and $\bar{t}$ masses must be equal. Of course there are complications, such as extra jets from initial and final state radiation, and also without (with) b-tagging there is an up to 24 (12) fold ambiguity in the assignment of jets. The kinematic fit is performed for all permutations and the best permutations (based on χ^2) are used to specify the fitted top mass. A maximum likelihood fit to a spectrum of fitted mass values of background and signal predictions for a range of hypothesized top quark masses finally yields a measurement of m_t . The largest uncertainties are due to the jet energy scale calibrations on the Monte Carlo event generators. Figure 5 shows as a representative of this method the DØ lepton+jets mass fit result.

The second method for measuring the top quark mass is to perform a kinematic fit to the all-jets events. Here the final state is measured completely and allows a three constraint fit. However the backgrounds are very large and so far only CDF, through the use of SVX b-tags to control background, reports a measurement of m_t with these events. Here the largest errors are again from jet energy scale calibrations and background modeling.

Finally both experiments report measurements of m_t from dilepton events.[24,25] Here only the sum of the transverse momenta of the two neutrinos is measured, yet

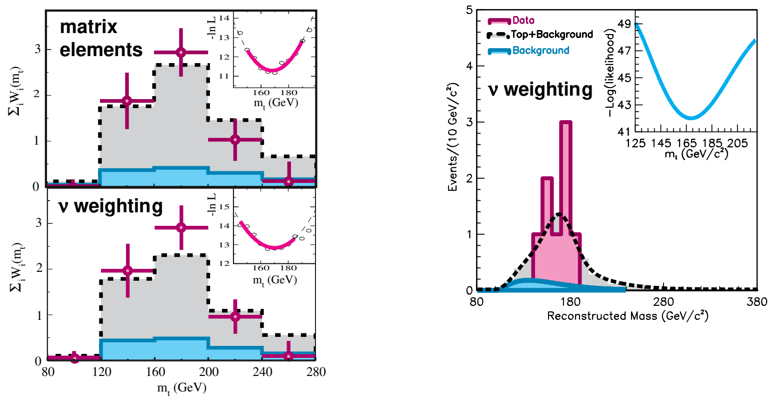

Fig. 6. Mass measurement results from the dilepton channel events for DØ (left, two methods) and CDF (right).

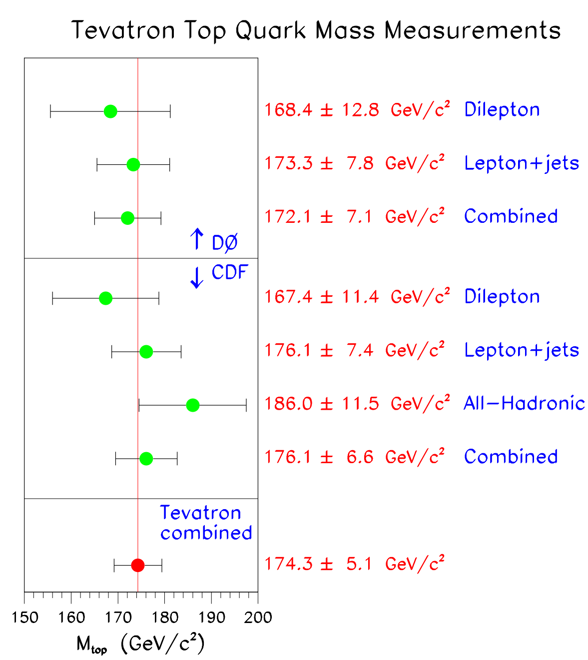

Fig. 7. Top mass measurements

there is extractable information about m_t within the event kinematics although these events are underconstrained and a kinematic fit as described above is not possible. In one analysis pioneered by DØ a dynamical likelihood method is employed where a weight function assigned to each events characterizes how likely it is that the event's kinematic variables would occur for a given range of top quark masses. These weight functions are then compared to Monte Carlo predictions to determine the most likely top mass. Figure 6 shows the results of this and another analysis from DØ and the similar analysis from CDF. With the present sample of dilepton channel events (six for DØ and eight for CDF) the statistical uncertainties are large. However this method has smaller systematic errors and will become competitive with the lepton+jets method in the Tevatron Run II despite the inherent differences in event statistics. Figure 7 summarizes and plots all five top quark mass measurements for both experiments. The results are all in good agreement within errors which further supports our claim that the signal that we see in the lepton+jets channel is indeed the same as the signal in the dilepton and all-jets channels and is that of $t\bar{t}$ decay.

3.4 The most precisely know quark mass: m_t

The CDF and DØ collaborations formed a working group to combine all the measurements of m_t to give a global Tevatron result. The systematic errors on the five mass measurements were each broken down into six components each with 22 subparts, and the correlations between the measurements were determined for each component separately. The final Tevatron Run I value of the top quark mass is: m_t = 174.3 $\pm$ 3.2 (stat) $\pm$4.0 (syst) GeV/c^2 = 174.3 $\pm$5.1 GeV/c^2. Figure 8 shows how the various measurements contribute to the central value. Most of the correlation is indirectly related to the jet multiplicity via the uncertainty on the jet energy scale calibration (the largest portion of systematic error for each).

The top quark now has the best measured mass of any quark with an uncertainty of only 2.9%. The top quark mass plays a major role in calculating predictions from the Standard Model via radiative corrections. It happens that the dominant radiative corrections to the W boson mass involve top quark and Higgs boson loops. Expressing the W boson mass as a tree-level value summed with a function of m_t and m_{Higgs}, we can constrain the mass of the Higgs boson within the framework of the Standard Model from precision measurements of m_t and m_W. Figure 9 shows the current best constraints on m_{Higgs} through a combination of the above value of m_t along with precision

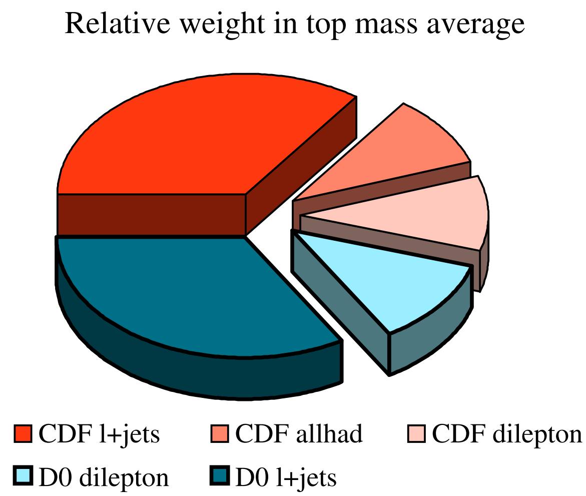

Fig. 8. The pie chart indicates the relative contribution of each measurement to the combined central value when correlations are taken into account.

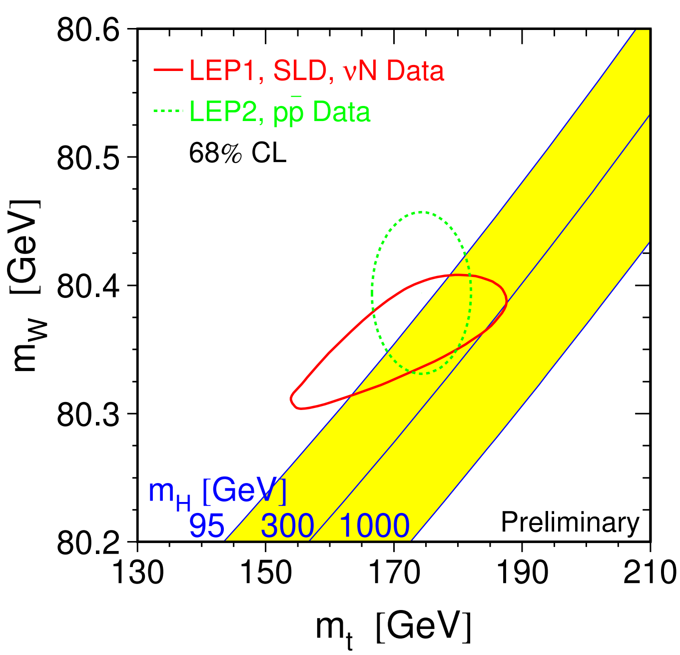

Fig. 9. Constraints on the Higgs mass in the m_W *vs.* m_t plane. The dotted ellipse is the 68% CL for Tevatron and LEP2 measurements.

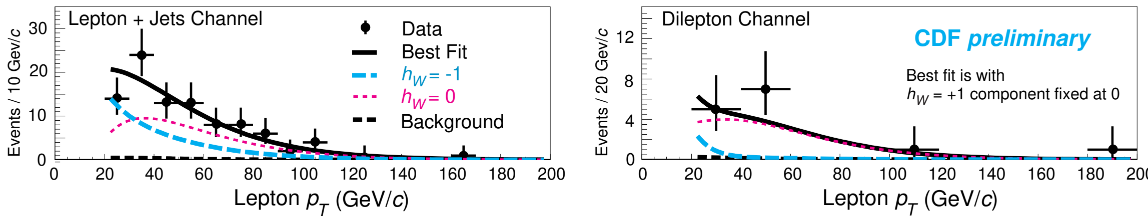

Fig. 10. Fits of W boson helicity fraction contributions to charged lepton p_T distribution in top quark decays.

measurements of electroweak parameters from around the globe.

4 Properties of $t\bar{t}$ Decay

We now turn our discussion to topics concerning the SM expectations of the decay of $t\bar{t}$ pairs. First is a description of an initial measurement of the helicity of the W in $t\bar{t}$ final states by CDF, and second we will examine a DØ analysis of spin correlations in $t\bar{t}$ decays.

4.1 Top Decay and Helicity of W Boson

As mentioned, a consequence of the top quark's extraordinarily heavy mass is that its primary decay channel is to a real W boson. Due to the V-A couplings in the electroweak sector of the SM, top can only decay to a longitudinally polarized (helicity $h_W = 0$) or left-handed ($h_W = -1$) W boson, and not to a right-handed helicity state. This well known phenomena of lepton decays has never been verified for the vector bosons themselves, until now. To leading order the decay ratio is:

$$\frac{B(t \to bW_{long})}{B(t \to bW_{left})} = \frac{1}{2}(\frac{m_t}{m_W})^2 = \frac{0.70}{0.30} = \frac{f_{long}}{f_{left}}$$

A study by the CDF collaboration uses the fact that the direction of the lepton from the W boson decay is correlated to the W boson's helicity state.[26] In the CDF analyses, a fit of the lepton p_T spectra for W decays in $t\bar{t}$ events, in both the lepton and dilepton channels, yields $f_{long} = 0.97 \pm 0.37 \pm 0.13$ (statistical and systematic uncertainties, respectively), in full agreement with the SM assuming the hypothesis of no right handed decays. The fits to lepton and dilepton top events are shown in Figure 10.

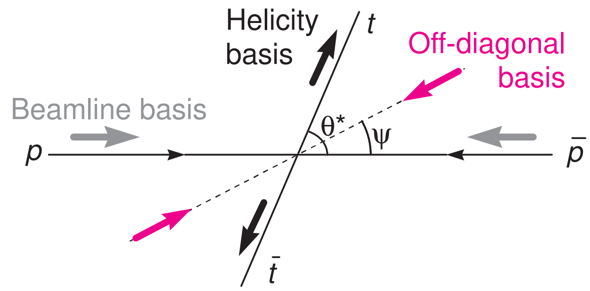

Fig. 11. Diagram of the off-diagonal basis, defined by the angle ψ relative to the beamline and the helicity basis (defined by θ_*).

4.2 W polarization and Top Pair Spin Correlation

In the Standard Model the spins of pair produced top quarks are correlated. Remarkably, the top quark lifetime ($\sim 4 \times 10^{-25}$ sec) is much shorter than the time required to hadronize, allowing information about top quark spin to be transmitted to their decay products. In this way the top's heavy mass allows a window to the spin of a bare quark!

For a polarized top quark, the angular distribution of the decay products in the top rest frame is given by:

$$\frac{1}{\Gamma}\frac{d\Gamma}{d\cos\theta} = \frac{(1+\alpha\cos\theta)}{2}$$

where $\alpha = 1$ for the charged lepton or d quark from the W decay, and $|\alpha| \leq 0.41$ for the other decay products (W, ν, b or the up quark). Unfortunately reconstructing down quarks from W boson decay is beyond current experimental analysis, so charged leptons offer the best means for extracting values of α. In addition, at the Tevatron top quarks are not polarized individually, and thus α cannot be measured in individual top decay. However, α can be determined from the correlated distribution in the decay angles θ_+ and θ_- of the t and $\bar{t}$:

$$\frac{1}{\sigma}\frac{d\sigma}{d\cos\theta_+ d\cos\theta_-} = \frac{1-\kappa\alpha_+\alpha_-\cos\theta_-\cos\theta_+}{4}$$

The value of κ depends on the axis of quantization chosen for the analysis of the decays. Note that the standard axes of the incident beam ('Gottfried-Jackson' frame) or the lines of flight of the top quarks ('helicity' frames) are not the ones preferred here. Instead Mahlon and Parke[27] have found that there is an optimal axis, or "off diagonal" basis, as defined by the transformation:

$$\tan\psi = \frac{\beta^{*2}\sin\theta^*\cos\theta^*}{1-\beta^{*2}\sin^2\theta^*}$$

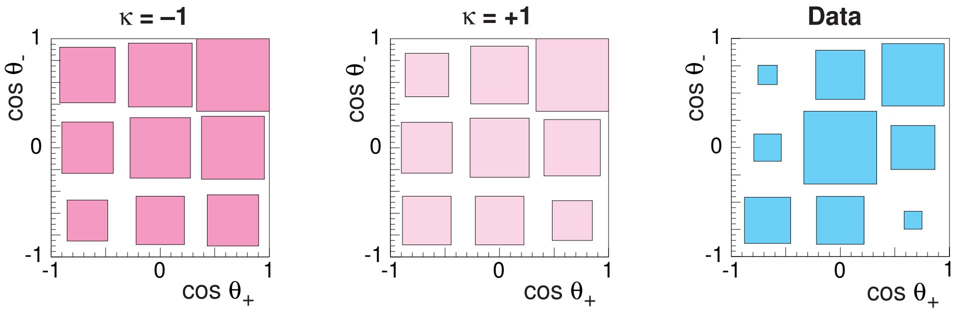

Fig. 12. Distributions for when the spins of the t and $\bar{t}$ are 100% anticorrelated, 100% correlated, and for data.

where ψ and θ^* are, respectively, the angle of the optimal axis and the angle for the line of flight of the top quarks, defined relative to the incident direction of the $\bar{p}$ in the parton-parton rest frame, and β^* refers to the velocity of the top quarks in that frame. In the off diagonal basis, the impact from opposite spin orientations of the top quarks (e.g., from gluon-gluon production) vanish to leading order in α_{strong}, providing an expected value of $\kappa \sim 0.9$. To measure the decay angles requires the full kinematic reconstruction of $t\bar{t}$ events. Unfortunately, dilepton events are kinematically underconstrained, and a special procedure was therefore developed at DØ[24] to handle the ambiguities and poor resolution brought about by the two missing neutrinos in these channels. Using the 6 dilepton $t\bar{t}$ candidates, the DØ analysis calculates all possible neutrino solutions, with smeared resolutions, and obtains a likelihood for each event permutation. These were summed for all events, and are shown in the density plot in Figure 12. A likelihood fit was then performed to signal (based on a spin-correlated $t\bar{t}$ Monte Carlo) and small sources of background, with κ as arbitrary parameter, which established that $\kappa > -0.25$ at 68% confidence.[28] This result is consistent with production through an intermediary gluon, where on the other hand a value of $\kappa \sim -1.0$ would correspond to an intermediary Higgs-like $J = 0$ boson.

5 Studies of Top Production

A priority in the search for new phenomena is to see if there are any competing or anomalous production contributions to our $t\bar{t}$ event samples. We present four analyses in this vein, including a search for single top production through electroweak processes, in which $t\bar{t}$ production is itself a major background! The topics covered in this next

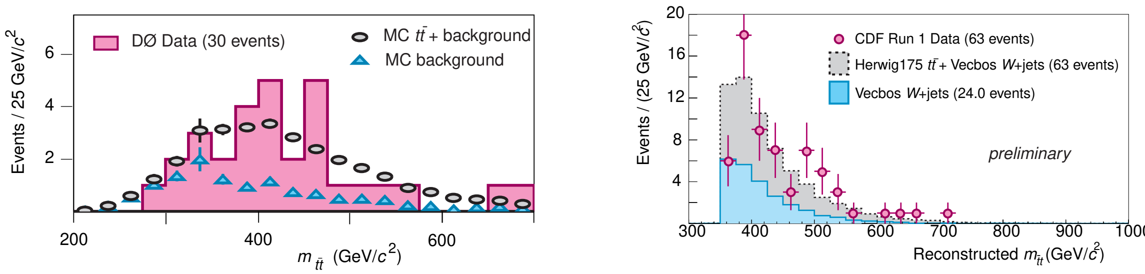

Fig. 13. Invariant mass distributions of the $t\bar{t}$ system for DØ (left) and CDF (right).

section are:

- Anomalous contributions to $t\bar{t}$ production from possible $m_{t\bar{t}}$ resonances
- Anomalous $t\bar{t}$ production and contributions to the p_T spectra of top quarks.
- Electroweak production of single top.
- Charged Higgs search through top "disappearance".

5.1 Invariant $t\bar{t}$ Mass

While the top quark lifetime is too short to permit any onium states it is still very interesting to look for possible resonances in the mass of the $t\bar{t}$ pair ($m_{t\bar{t}}$). Figure 13 contains invariant $m_{t\bar{t}}$ spectra for DØ and CDF lepton+jet events. The spectrum from the DØ events uses a 2C fit to the same events used in the mass fit. To the right of this plot is the spectrum from CDF events with an additional constraint that the top mass m_t = 175 GeV/c^2. In addition CDF applies a cut on the fit χ^2 as well as selection criteria to optimize sensitivity to new physics by reducing combinatoric backgrounds from wrong jet combinations. Neither experiment sees any significant excess with these statistics.

5.2 Transverse Momentum of Top Quarks in $t\bar{t}$ Production

Anomalous $t\bar{t}$ production through a high mass intermediate particle could also show up in the p_T spectrum of the top quark. Some extended Technicolor models predict an enhancement of the SM at high p_T . Using the measured value of m_t and event fitting techniques developed for the mass measurement, a 3C fit can be made for the p_T of the each top in lepton+jets events. CDF[30] has performed such a study and the results are shown in Figure 14 with the top quark p_T in four 75 GeV wide bins. These models predict an excess in bin 4, and the data is in excellent agreement with the SM within current statistics.

Top Quark Differential Cross Section

$$R_1 + R_2 = 0.72^{+0.13}_{-0.13}(\text{stat})^{+0.06}_{-0.06}(\text{syst})$$
$$R_4 < 0.114 \text{ at } 95\% \text{ C.L.}$$

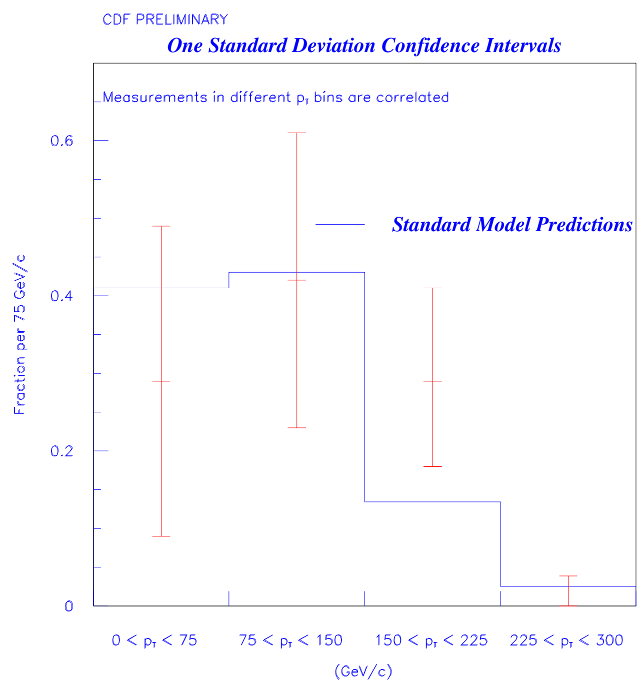

p_T Bin	Measured Fraction of Top Quarks
$0 < p_T < 75$ GeV/c	$R_1 = 0.29^{+0.18}_{-0.18}(\text{stat})^{+0.08}_{-0.08}(\text{syst})$
$75 < p_T < 150$ GeV/c	$R_2 = 0.42^{+0.18}_{-0.18}(\text{stat})^{+0.05}_{-0.07}(\text{syst})$
$150 < p_T < 225$ GeV/c	$R_3 = 0.29^{+0.12}_{-0.10}(\text{stat})^{+0.06}_{-0.05}(\text{syst})$
$225 < p_T < 300$ GeV/c	$R_4 = 0.000^{+0.035}_{-0.000}(\text{stat})^{+0.019}_{-0.000}(\text{syst})$

Fig. 14. The p_T distribution of top quarks in $t\bar{t}$ events from CDF. R_n is the fraction of events in p_T bin n.

5.3 Electroweak Production of Single Top

At the Tevatron, top quarks can also be produced singly via the electroweak interaction.[31] The electroweak production of top is predominantly through two processes involving off shell W boson exchange and the SM cross section for each is about 1pb. The tree level Feynman diagrams for the two most important processes are shown in Figure 15. CDF has performed a search for single top in 109 pb^{-1} of data. The search strategy is to look for events with an isolated high p_T electron or muon and associated significant missing E_T of a neutrino from the W decay, and exactly two jets, with one or both jets tagged as a b-quark using the displaced vertex method of b-tagging. In addition, the reconstructed invariant top quark mass must fall within $145 < m_T < 205$ GeV.

The signal from single top production is more challenging to separate from the major background of W + jets events than the signal from $t\bar{t}$ production. In fact $t\bar{t}$ production is a major background to this process. Higher background rates together with a smaller cross section prevents detection of this process with current statistics. However, CDF does set upper limits on the cross sections for these two processes. Figure 16 contains distributions of modeled background, sum of signal and background, and data, for the reconstructed top mass (for s-channel analysis) and for the quantity 'lepton charge $\times$ untagged jet pseudorapidity'(for the t-channel analysis). This second quantity takes advantage of decay kinematics in that the light quark tends to be emitted along the direction of the top quark. From likelihood fits to these distributions the following upper limits are reported by CDF[32]:

$$\sigma(p\bar{p} \to t\bar{b}, \bar{t}b) < 15.8 \text{ pb at 95\% C.L.}$$

$$\sigma(p\bar{p} \to tq\bar{b}, \bar{t}\bar{q}b) < 15.4 \text{ pb at 95\% C.L.}$$

5.4 Charged Higgs Search Through Top "Disappearance"

In supersymmetric extensions of the Standard Model the top quark has another decay option, $t \to H^+b$, in addition to the standard decay $t \to Wb$. This is allowed in the two Higgs doublet models, the phenomenology of which is characterized by two parameters: the mass of the charged Higgs boson, m_{H^+}, and the ratio of the vacuum expectation values of the two Higgs doublets, $\tan\beta$. The model predicts that when $\tan\beta$ is larger or smaller than $\tan\beta = \sqrt{m_t/m_b} \sim 6$ the decay to the charged Higgs

Fig. 15. Leading order Feynman diagrams for W^* single top production and W-gluon fusion at the Tevatron.

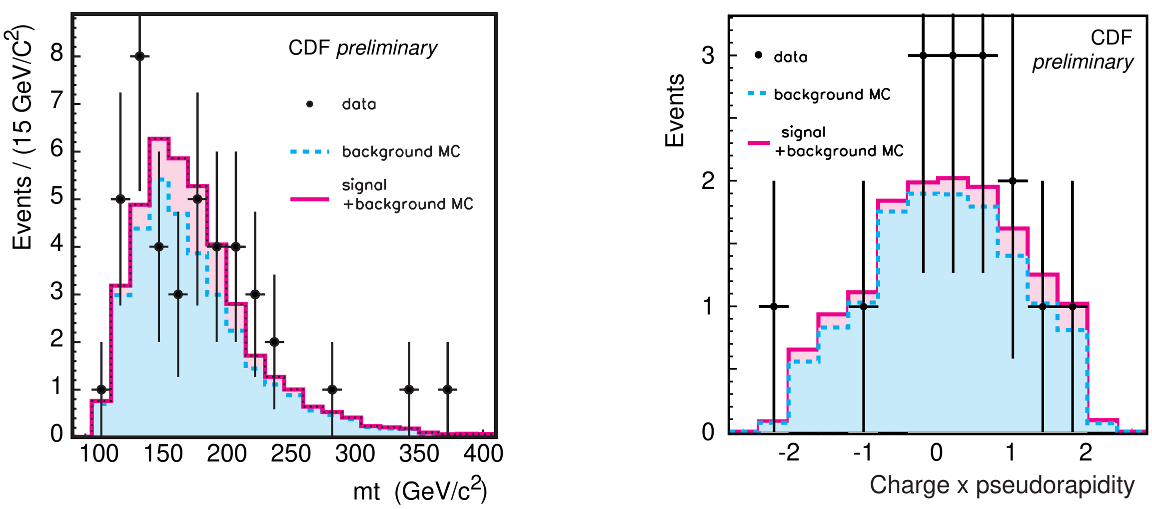

Fig. 16. The left plot is the reconstructed top mass distribution for s-channel single top production, and the right plot is the lepton charge $\times$ untagged jet pseudorapidity for t-channel single top production.

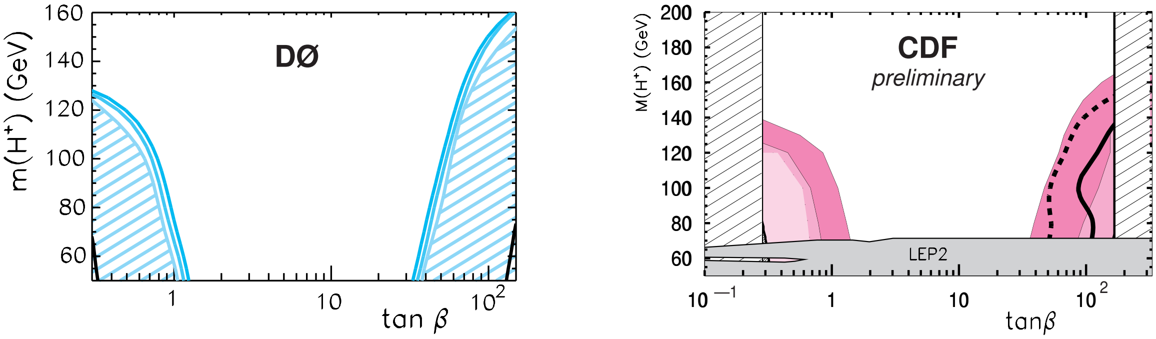

Fig. 17. Exclusion regions in the ($\tan\beta$, m_{H^+}) plane.

will dominate. At very large $\tan\beta$ the charged Higgs will decay predominantly to tau leptons ($H^+ \to \tau\nu$), and for small $\tan\beta$ the charged Higgs will decay mostly through hadronic channels ($H^+ \to c\bar{s}$ or $H^+ \to t^*\bar{b} \to Wb\bar{b}$, depending on m_{H^+}).

Both CDF[33] and DØ[34] have performed what we have termed 'disappearance' analyses in which we determine how much phase space is left for decays after all reconstructed $t \to Wb$ decays are taken into account. Here the inherent inefficiencies of our detectors for finding $t \to \tau\nu$ and $t \to c\bar{s}$ is turned to an advantage; similar decays from H^+ would also be invisible but would impact the number of top events expected by the SM in our most efficient channels. Figure 17 shows results of searches for such deficits relative to SM expectations, expressed as a limits in $\tan\beta$, m_{H^+} parameter space. The hatched regions in the DØ plot and the solid regions in the CDF plot are excluded at the 95% confidence level. The three lines at the limiting boundary of the DØ plot are for different values of the $t\bar{t}$ cross section, 5.5, 5.0 and 4.5 pb. The tightest limit on the CDF plot corresponds to 5.0 pb, and the next is 7.5 pb (close to the CDF measured value).

CDF has also performed direct searches for the top decay channel ($t \to \tau\nu$),[35] and can set direct limits on charged Higgs production at high $\tan\beta$. The solid and broken lines indicate limits set for cross sections of 5.0 and 7.5 pb. The CDF plot also indicates the $\tan\beta$ independent limit $m_{H^+} > 60$ GeV set by direct searches at LEP.

6 Conclusions

The first run of the Tevatron collider allowed the top quark to become the best measured of any of the known quarks, and we have had a successful first pass at developing the analyses to measure many properties of the top quark and its decay. Table 2 details some of the current measurements and indicates projections for the Run II of the Tevatron based on the increased luminosity and improved detector capability. Overall the outlook for top physics at the Tevatron Run II is very bright.

Table 2. Projections for Tevatron Run II top measurements with 2 fb^{-1} of integrated luminosity.

Top Quark Property	Run I measurement	Precision Run I	Precision Run II
$\sigma_{t\bar{t}}$ (DØ)	$5.9^{+1.7}_{-1.7}$	25%	10%
$\sigma_{t\bar{t}}$ (CDF)	$6.5^{+1.7}_{-1.4}$		
m_t (DØ)	$172.1 \pm 5.2 \pm 4.9$ GeV/c^2		
m_t (CDF)	$176.1 \pm 4.2 \pm 3.1$ GeV/c^2	3.8%	1.7%
m_t (DØ + CDF)	$174.3 \pm 3.3 \pm 3.9$ GeV/c^2	2.9%	1.2%
W helicity F_{long}	$0.91 \pm 0.37 \pm 0.13$	0.4	0.09
$\sigma_{single-top}$	< 18.6 pb	-	20%
$\Gamma(t \to Wb)$	-	-	25%
$\lvert V_{tb} \rvert$	-	-	12%
BR($t \to \gamma q$) 95% CL	0.03	0.03	0.002
BR($t \to Z^0 q$) 95% CL	0.30	0.30	0.02

7 Acknowledgements

I wish to thank my colleagues on CDF and DØ for their many contributions that have provided the basis for this presentation. I am especially grateful to Ann Heinson (especially for the supply of some graphics), Tom Ferbel, Mark Kruse, John Conway, and Gordon Watts for their input and helpful comments. I thank both David Burke and Lance Dixon for the invitation and immense honor of participating in the SLAC Summer Institute 2000 and I express my appreciation to conference administrator Ellie Lwin for all her gracious help with my conference arrangements.

References

[1] S.W. Herb *et al.*, Phys. Rev. Lett. **39**, 253 (1977)

[2] G. S. Abrams *et al.*, Phys. Rev. Lett. **63**, 2447 (1989).

[3] D. Decamp *et al.* [ALEPH Collaboration], Phys. Lett. **B236**, 511 (1990). P. Abreu *et al.* [Delphi Collaboration], Phys. Lett. **B242**, 536 (1990). M. Z. Akrawy *et al.* [OPAL Collaboration], Phys. Lett. **B236**, 364 (1990). O. Adriani *et al.* [L3 Collaboration], Phys. Lett. **B313**, 326 (1993).

[4] R. Marshall, Z. Phys. **C43**, 607 (1989).

[5] V. Barger and S. Pakvasa, Phys. Lett. **B81**, 195 (1979). G. Eilam, A. Soni, G. L. Kane and N. G. Deshpande, Phys. Rev. Lett. **57**, 1106 (1986).

[6] A. Bean *et al.* [CLEO Collaboration], Phys. Rev. D **35**, 3533 (1987).

[7] D. P. Roy and S. Uma Sankar, Phys. Lett. **B243**, 296 (1990).

[8] H. Albrecht *et al.* [ARGUS Collaboration], Phys. Lett. **B324**, 249 (1994). J. Bartelt *et al.* [CLEO Collaboration], Phys. Rev. Lett. **71**, 1680 (1993).

[9] [ALEPH Collaboration], CERN-PPE-94-187 *Contributed to the 27th International Conference on High-Energy Physics - ICHEP 94, Glasgow, Scotland, UK, 20 - 27 Jul 1994*.

[10] F. Abe *et al.* [CDF Collaboration], Phys. Rev. Lett. **74**, 2626 (1995) [hep-ex/9503002].

[11] S. Abachi *et al.* [D0 Collaboration], Phys. Rev. Lett. **74**, 2632 (1995) [hep-ex/9503003].

[12] S. Abachi *et al.* [D0 Collaboration], Nucl. Instrum. Meth. **A338**, 185 (1994).

[13] F. Abe *et al.* [CDF Collaboration], Nucl. Instrum. Meth. **A271**, 387 (1988).

[14] D. Amidei *et al.* [CDF Collaboration], Nucl. Instrum. Meth. **A350**, 73 (1994).

[15] R. L. Wagner [CDF COLLABORATION Collaboration], Nucl. Instrum. Meth. **A265**, 1 (1988).

[16] S. Abachi *et al.* [D0 Collaboration], Phys. Rev. Lett. **79**, 1203 (1997) [hep-ex/9704015].

[17] F. Abe *et al.* [CDF Collaboration], Phys. Rev. Lett. **80**, 2773 (1998) [hep-ex/9710008].

[18] F. Abe *et al.* [CDF Collaboration], Phys. Rev. Lett. **79**, 3585 (1997) [hep-ex/9704007].

[19] B. Abbott *et al.* [D0 Collaboration], Phys. Rev. D **60**, 012001 (1999) [hep-ex/9808034].

[20] F. Abe *et al.* [CDF Collaboration], Phys. Rev. Lett. **79**, 1992 (1997).

[21] E. Laenen, J. Smith, and W.L. van Neerven, Phys. Lett. B **321**, 254 (1994); E.L. Berger and H. Contopanagos, Phys. Rev. D **54**, 3085 (1996); S. Catani *et al.*, Phys. Lett. B **378**, 329 (1996); R. Bonciani *et al.*, Nucl. Phys. B **529**, 424 (1998).

[22] S. Abachi *et al.* [D0 Collaboration], Phys. Rev. Lett. **79**, 1197 (1997) [hep-ex/9703008].

[23] F. Abe *et al.* [CDF Collaboration], Phys. Rev. Lett. **80**, 2767 (1998) [hep-ex/9801014].

[24] B. Abbott *et al.* [D0 Collaboration], Phys. Rev. Lett. **80**, 2063 (1998) [hep-ex/9706014].

[25] F. Abe *et al.* [CDF Collaboration], Phys. Rev. Lett. **82**, 271 (1999) [hep-ex/9810029].

[26] T. Affolder *et al.* [CDF Collaboration], Phys. Rev. Lett. **84**, 216 (2000) [hep-ex/9909042].

[27] G. Mahlon and S. Parke, Phys. Lett. **B411**, 173 (1997) [hep-ph/9706304].

[28] B. Abbott *et al.* [D0 Collaboration], Phys. Rev. Lett. **85**, 256 (2000) [hep-ex/0002058].

[29] T. Affolder *et al.* [CDF Collaboration], Phys. Rev. Lett. **85**, 2062 (2000) [hep-ex/0003005].

[30] T. Affolder *et al.* [CDF Collaboration], FERMILAB-PUB-00-101-E.

[31] T. Stelzer, Z. Sullivan and S. Willenbrock, Phys. Rev. D **58**, 094021 (1998) [hep-ph/9807340].

[32] T. Kikuchi, S. K. Wolinski, L. Demortier, S. Kim and P. Savard [CDF Collaboration], FERMILAB-CONF-00-290-E *Presented at DPF 2000, Columbus, Ohio, 9-12 Aug 2000.*

[33] F. Abe *et al.* [CDF Collaboration], Phys. Rev. Lett. **73**, 2667 (1994).

[34] B. Abbott *et al.* [D0 Collaboration], Phys. Rev. Lett. **82**, 4975 (1999) [hep-ex/9902028].

[35] F. Abe *et al.* [CDF Collaboration], Phys. Rev. D **54**, 735 (1996) [hep-ex/9601003]. T. Affolder *et al.* [CDF Collaboration], Phys. Rev. D **62**, 012004 (2000) [hep-ex/9912013].